Scientific Research Publishing

Materials Sciences and Applications, 2025, 16(1), 1-10
https://www.scirp.org/journal/msa
ISSN Online: 2153-1188
ISSN Print: 2153-117X

Phase-Field Modeling of the Rearrangement Process of Foam Structures Considering Pressure Effects

Takuya Uehara

Department of Mechanical Systems Engineering, Yamagata University, Yonezawa, Japan
Email: uehara@yz.yamagata-u.ac.jp

How to cite this paper: Uehara, T. (2025) Phase-Field Modeling of the Rearrangement Process of Foam Structures Considering Pressure Effects. *Materials Sciences and Applications*, **16**, 1-10.
https://doi.org/10.4236/msa.2025.161001

Received: December 13, 2024
Accepted: January 23, 2025
Published: January 26, 2025

Abstract

Foam structures have been attracting many scientists for a long time. However, the physics behind these structures is very complicated, and complete modeling has not yet been achieved. In this paper, a phase-field modeling of the rearrangement process of foam structures was proposed, and simulations were conducted to show its effectiveness. Adjacent foam cells were assumed to interact with each other through the pressure difference, and four different conditions were introduced. When the cells had identical inner pressures at the initial state, they were stabilized, keeping the initial volume. In contrast, a volumetric change occurred when the amount of the substance in the initial cells was provided. Other models to regenerate small-cell distribution were also proposed, and the foam structures observed in real liquid foam were successfully reproduced.

Keywords

Phase-Field Model, Foam, Microstructure, Thermodynamics, Finite-Difference Method, Computer Simulation

1. Introduction

Various foam structures are prevalent in everyday life, and they are utilized in various engineering fields. For example, porous metallic materials called metal foams have excellent advantages in terms of their light weight against normal metals and in terms of their strength against polymers [1]. Additionally, their cellular voids produce various functionalities such as sound absorption, thermal insulation, and vibration reduction [2]. These material properties depend not only on the species of the base material but also on its geometric characteristics, such as the shape and

size of each cell and their arrangement. Therefore, optimizing the microstructure of these materials is desirable to maximize their functionality. To make this possible, the relationship between functional properties and microstructures should be clarified. However, even for ideal structures, such as regularly arranged homogeneous polyhedrons, making up cells artificially one by one is not realistic. Practically, solid foam materials are often processed from liquid foam, which can be observed in soap or beer: the foam is generated in the liquid base, and then solid porous materials are obtained through solidification processes, and the liquid foam structure is frozen into a solid foam material. Therefore, in these cases, the stabilizing process of each cell leading to the final cell distribution should be investigated [3] [4].

Many researchers, starting from Plateau in the late 19th century, have investigated the shape of the liquid foam; a translated octahedron, known as a Kelvin cell, is considered the most preferable shape [5]. However, real foam does not always consist of Kelvin cells but is usually made up of various shapes. Additionally, time-dependent coarsening or destruction makes the problem more complicated, and the modeling of foam structures is still under investigation [6]-[8]. Nevertheless, the microstructures of porous materials can be designed if the stabilized shape of each cell and its distribution in the whole structure are predicted. However, experimental observations have limitations in fully understanding these structures because of their complexity.

In this regard, computer simulation has become a powerful and effective tool. For instance, Weaire and Phelan found a better form of the space-filling polyhedral model using computer simulations [9]. However, although such a geometrically optimum structure was obtained, the real foam structure could not be reproduced because various physical, chemical, and, sometimes, electromagnetic factors dominated the structure [10]. For these complex problems, an ambiguous model is sometimes more useful. In this respect, previous studies reported a simulation model to represent the foam structure using a phase-field model [11]-[13], which reproduced the growth of cells from nuclei and the formation of the foam pattern. A stabilized structure was also generated by applying the volume-control term, but the situation where the volume difference in the adjacent cell dominated the growth rate was unrealistic. Thus, in this paper, the volume-control term is substituted by the pressure-control term to improve the previous model. Four different types of models are introduced to the initiation of the cells, which allows for variation in the inner pressure, and the stabilized foam structure is discussed.

2. Phase-Field Model and Fundamental Equations

2.1. Multi-Phase-Field Model

The conventional phase-field model expresses two different phases using a single phase-field variable, ϕ, which varies from 0 to 1 continuously but steeply in the interfacial region. The multi-phase-field model [14] [15] is modified to express multiple phases using ϕ_i, where the suffix i represents the i-th phase and ϕ_i

varies by maintaining

$$\sum_{i=1}^{N}\phi_i = 1 \tag{1}$$

where N is the total number of phases considered. In this paper, the foam structure is considered as an assembly of multiple cells, and ϕ_i is assigned to the i-th foam cell. Then, the cell wall corresponds to the interface of the neighboring cells.

2.2. Fundamental Equations

The fundamental equation of the multi-phase-field model in the following form is applied.

$$\frac{\partial \phi_i}{\partial t} = -\frac{2}{n}\sum_j m_{ij}\left(f_{ij}^{g} + f_{ij}^{p} + f_{ij}^{c}\right) \tag{2}$$

where, f_{ij}^{g}, f_{ij}^{p}, and f_{ij}^{c} are respectively expressed as:

$$f_{ij}^{g} = \sum_k \frac{1}{2}\left(a_{ik}^2 - a_{jk}^2\right)\nabla^2\phi_k,\quad f_{ij}^{p} = \sum_k \left(w_{ik} - w_{jk}\right)\phi_k,\quad f_{ij}^{c} = \Delta f_{ij}\sqrt{\phi_i\phi_j} \tag{3}$$

where m_{ij}, a_{ij}, w_{ij}, and Δf_{ij} are the parameters depending on the combination of the i-th and j-th phases. The variation in ϕ_i is expressed in relation to the other phase field value ϕ_i, where j is generally all cells excluding i itself but actually includes only j of the adjacent cells. In Equation (2), n is the total number of the effective phase fields out of the total number N. In a previous model [13], an additional term

$$f_{ij}^{V} = K_{ij}^{V}\left(V_j - V_i\right)\left|\nabla\phi_i\right|^2\left|\nabla\phi_j\right|^2 \tag{4}$$

was added, where V_i is the volume of the cell represented by ϕ_i and K_{ij}^{V} is the adjusting parameter. The volume is successfully controlled by this term, but the situation where the volume difference dominates the growth rate is not based on a physical standpoint. Instead, in this paper, this term is substituted by a pressure-induced term in the following form:

$$f_{ij}^{p} = K_{ij}^{p}\left(p_j - p_i\right)\left|\nabla\phi_i\right|^2\left|\nabla\phi_j\right|^2 \tag{5}$$

where p_i is the internal pressure of the i-th cell and K_{ij}^{p} is the adjusting parameter. The pressure p_i varies as volume changes. Assuming the state equation of the ideal gas, the following relation holds:

$$p_i = n_i RT/V_i \tag{6}$$

where n_i is the amount of substance in the i-th cell, R is the gas constant, and T is the temperature. Considering the generation process of a foam cell, two cases are assumed: the initial pressure is constant or the initial amount of the substance is given. In this study, three different types are considered.

Type 1: $p_i = p_0$ for all cells.

Type 2: $n_i = n_0$ for all cells.

Type 3: n_i = random for each cell ($n_0^{\max} > n_i > n_0^{\min}$).

Following Equation (6), the pressure in a cell becomes infinitely large when the cell shrinks to vanish. A limit value V_{th} is set to avoid this.

In addition, observing real foam, small cells sometimes stabilize at a certain size. To achieve this situation,

$$p_i = k\left(V_{st} - V_i\right) \text{ for } V_i \langle V_{st},\ 0 \text{ for } V_i \rangle V_{st} \tag{7}$$

is used instead of Equation (6), expecting the shrinking cell to stabilize around the size of V_{st}, and the result is presented as Type 4. This effect may be caused by the balance of the internal pressure and surface tension, although a detailed discussion is left for future work.

3. Model and Conditions

3.1. Simulation Model

The phase-field equation is differentiated in the three-dimensional space using the finite difference method. The simulation box was set to 100 × 100 × 20 in size, and periodic boundary conditions were applied in all directions. One direction (z) was set thin so that the change in shape and size of every cell was visible. Generally, phase-field simulation is possible for generating foam structures by simulating cell growth from small nuclei. However, in this study, only the morphological change starting from a given structure was focused on. Voronoi tessellation with random seeds was applied to make the initial configuration, and the divided pattern is shown in Figure 1. The colors indicate the identification numbers of the cells, which are randomly provided from 1 to N (=20), corresponding to i of ϕ_i, where N is the total number of cells.

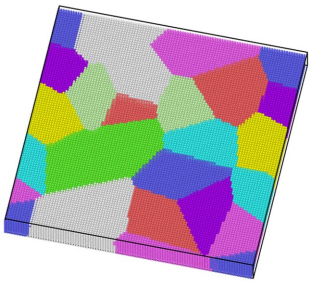

Figure 1. Simulation model and the initially divided cell pattern.

3.2. Parameters and Conditions

The computational and phase-field parameters are listed in Table 1. All values are standardized nondimensional values. Conditional values such as p_0 and n_0 are varied, and typical results are presented in the following section. The parameters including the suffix ij generally depend on the combination of the phases i and j; however, in this study, identical values are used for all ij. The parameter Δf_{ij} is the difference in the chemical potential of the phases and is effective for phase transformation. In this study, this term is neglected as the initial state is assigned after the transformation is completed.

Table 1. Computational and phase-field parameters.

Δx	Δt	m_{ij}	a_{ij}	w_{ij}	Δf_{ij}
0.15	0.004	1.0	1.0	4.93	0.0
K_{ij}^{p}	V_{th}	RT			
1.0	$100\,\Delta x^3$	1.0			

4. Results and Discussion

4.1. Type 1

Figure 2 represents the variation of the cell distribution using the conventional multi-phase-field model without f^{V} or f^{p}. At the early stage, from the initial step toward the 400th timestep, as shown in Figure 2(a) and Figure 2(b), sharp angles tended to broaden, and too-close junctions tended to separate, which is a natural behavior of the phase-field model. As time passed, larger cells grew larger and smaller cells shrank until they vanished, and the number of cells decreased. The initially assigned 20 cells decreased to four cells at the 10000th timestep, as shown in Figure 2(f), leading to a single crystal if the calculation was continued.

Figure 3 represents the result obtained when the additional term f^{p} and Type-1 condition with $p_0 = 0.1$ were applied. The initial volume of each cell was different, but the pressure was set the same. Therefore, every cell changed its shape by maintaining its volume. In the early stage, as shown in Figure 3(a) and Figure 3(b), relaxation in sharp angles occurred, as in the case shown in Figure 2. Thereafter, only the change in shape occurred to form a hexagonal shape, and most intersections of the cells became triple junctions consisting of 120˚ angles, as shown in Figure 3(c). The whole structure reached a stable state, and no specific change was observed after the 2000th timestep, as shown in Figures 3(d)-(f).

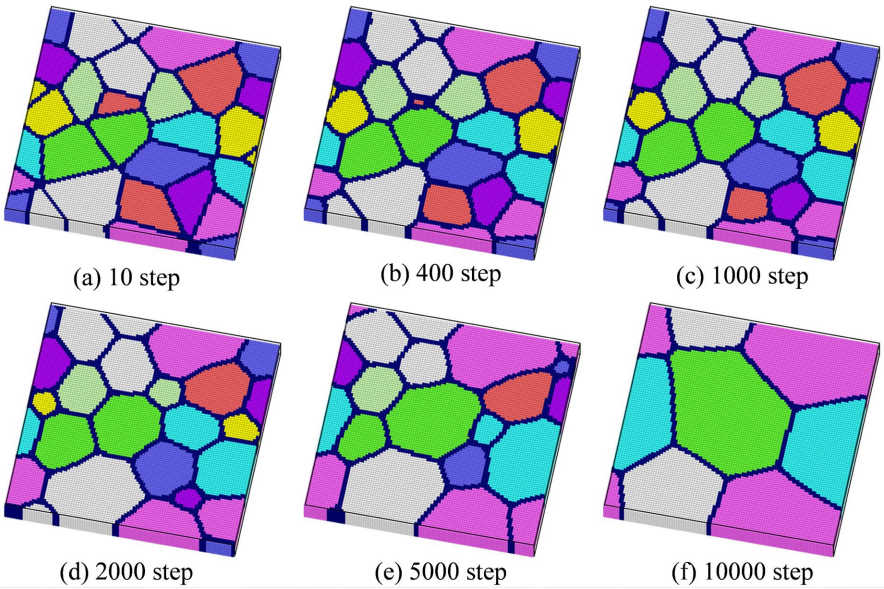

Figure 2. Variation of the cell shape using the conventional multi-phase-field model.

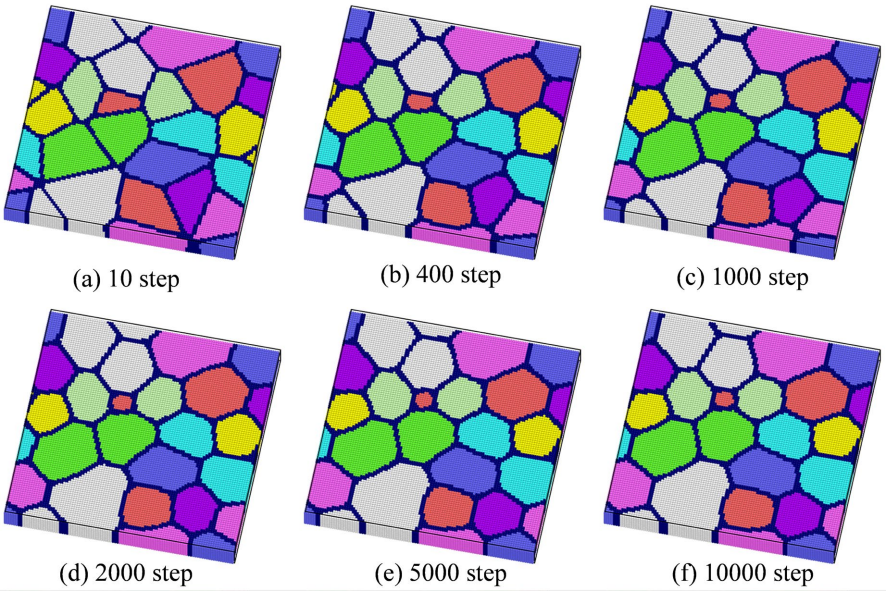

Figure 3. Variation of the cell shape under the Type-1 condition.

4.2. Type 2

Figure 4 represents the variation in cell distribution using the Type-2 condition with $n_i = 8.4$. In this case, the same amount of substance was assumed to be contained in every cell, corresponding to high pressure in small cells and low pressure inlarge cells. Because of the effect of the term f^p on Equation (2), alternation in volume occurred to make the pressure of the adjacent cells equal. A typical difference between Types 1 and 2 was observed in a cell depicted in red and indicated by an arrow in Figure 4(a). The cell remained small in Type 1, as shown in Figure 3. In contrast, the cell grew larger in Type 2, as shown in Figure 4. At the same time, with volume change, the adjustment in shape progressed, and the cell became hexagonal. Its edge lengths were also adjusted, and the final form was close to that of a regular hexagon, as shown in Figure 4(f). All cells behaved similarly, and it finally reached a stable state. Note that several other shapes were retained because of the restriction by the periodic boundary.

The variations of the cell size and pressure are shown in Figure 5(a) and Figure 5(b), respectively. The blue and red lines are the results for Types 1 and 2, respectively, and the solid and dashed lines are the maximum and minimum values in cell size or pressure, respectively. The difference in the maximum and minimum cell sizes was small for Type 2, which denoted that most cells had almost equal sizes, whereas various cell sizes were distributed in Type 1. As the initial condition, the pressure was set to be the same for Type 1 but varied for Type 2. In Figure 5(b), the difference in the maximum and minimum values was larger in Type 1 than in Type 2. This was because the term f^p worked in cooperation with the other terms in Equation (2). As the native tendency of the phase field, the cell size moved to separate, as shown in Figure 2. Thus, the balanced size of each cell was slightly different depending on the shape or state of the adjacent cells. In any case,

variation occurred in the early stage, and stable states were accomplished by the effect of f^p.

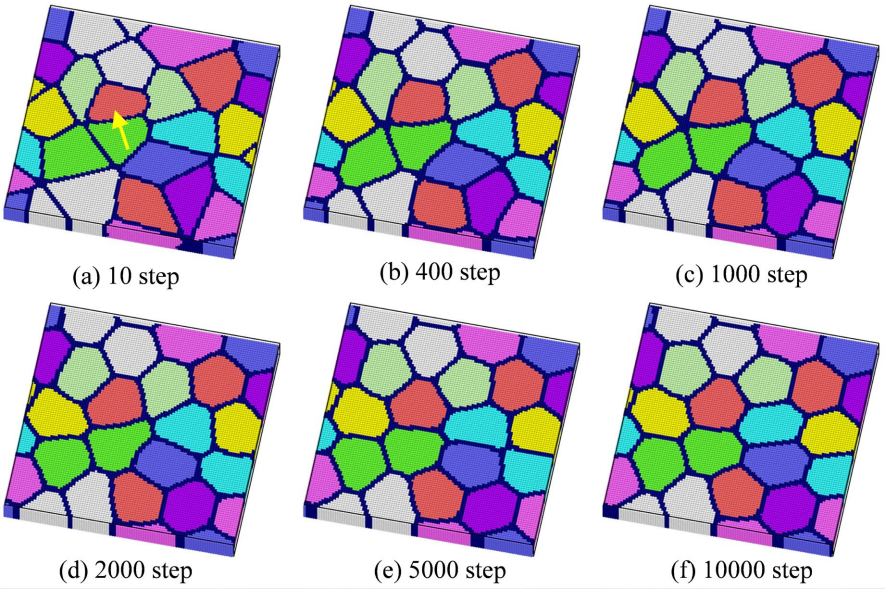

Figure 4. Variation of the cell shape under the Type-2 condition.

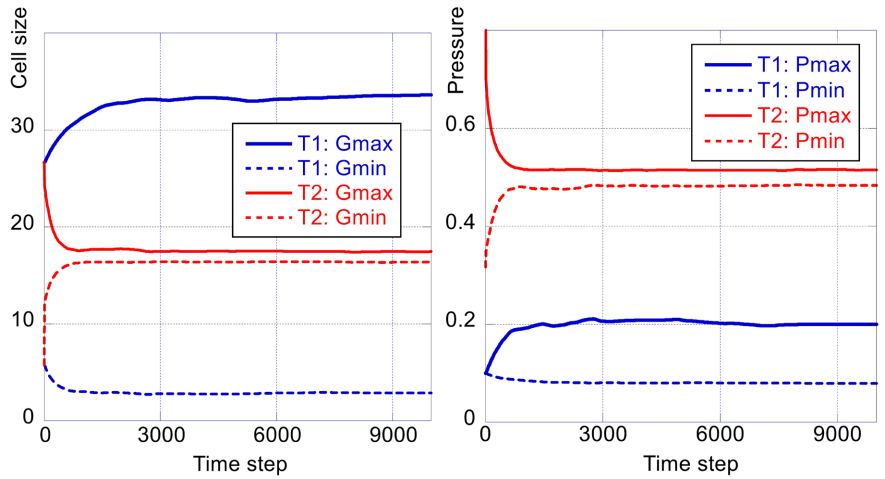

(a) Cell size (b) Pressure

Figure 5. Variation of the cell size and pressure for Types 1 and 2.

4.3. Type 3

The Type-3 condition was basically the same as Type 2, but the amount of substance in each cell was provided randomly. **Figure 6** represents the result for Type 3 with $n_0^{\min} = 0.42$ and $n_0^{\max} = 3.16$. Depending on the initial contents of the substance, the internal pressure varied for every cell. Consequently, variously sized cells were distributed in the stable state, as shown in **Figure 6(f)**. The shape was mostly hexagonal, whereas the ratio of other shapes, such as pentagons or seven- or eight-sided shapes, increased compared with that in **Figure 4**.

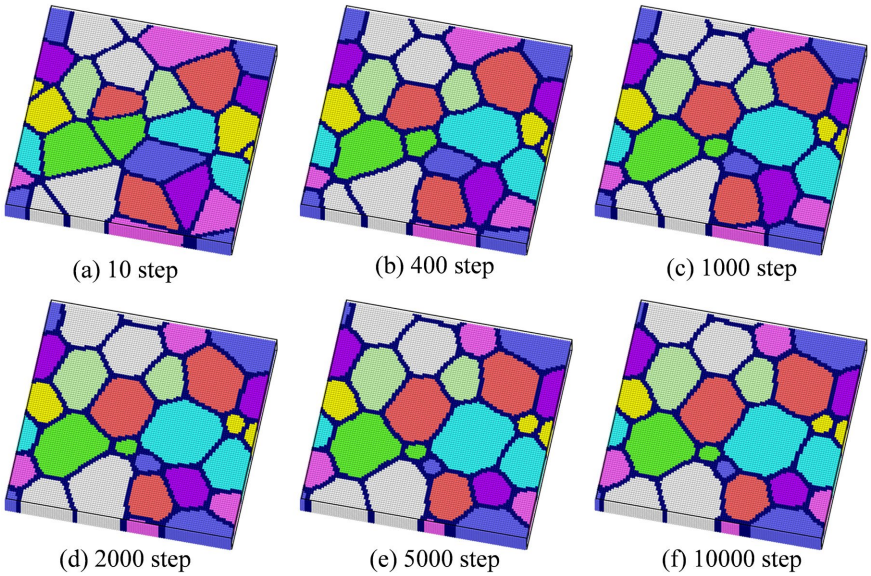

Figure 6. Variation of the cell shape under the Ttype-3 condition.

4.4. Type 4

The Type-4 condition was intended to prevent reduced cells from vanishing completely. The simulation result for $k = 10.0,\ V_{st} = 500\Delta x^3$ is presented in Figure 7. Initially, small cells started shrinking at first, as shown in Figure 7(a) and Figure 7(b). However, the shrunk cells, such as the cell denoted by the arrow, did not further shrink and remained afterward, as shown in Figures 7(c)-(f). Other diminishing cells also stopped shrinking and remained at a certain size. Consequently, small cells remained without disappearing, as shown in Figure 7(f). A similar pattern is often observed in real liquid foam, and the model is considered to reflect real phenomena.

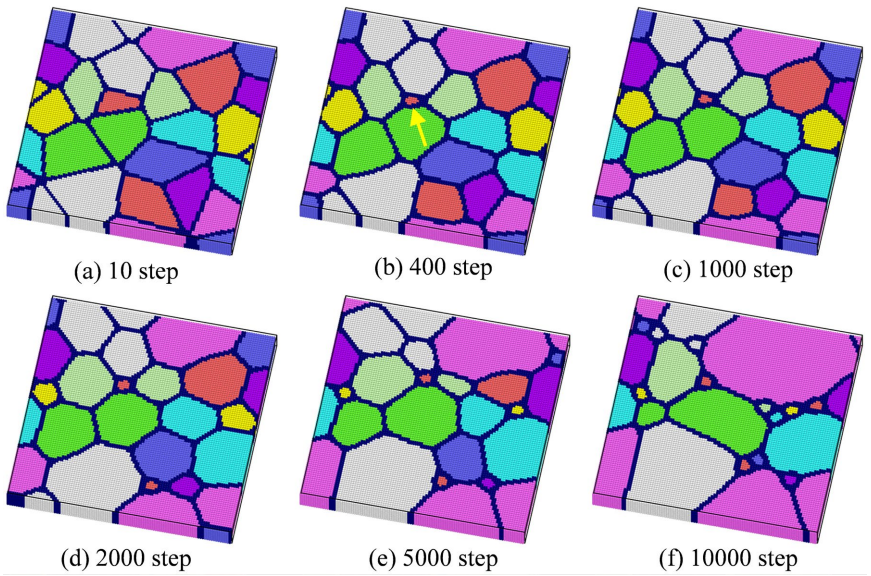

Figure 7. Variation of the cell shape under the Ttype-4 condition.

5. Conclusions

In this paper, the phase-field modeling of the rearrangement process of foam structures was presented. Adjacent foam cells were assumed to interact with each other through pressure difference. Simulations were conducted under different conditions, and the following results were obtained. When the cells had identical inner pressures at the initial state, they stabilized and maintained their initial volume. In contrast, a volumetric change occurred when the amount of the substance in the cells was provided. Another model to regenerate the small cell distribution was also proposed, and the foam structure observed in real liquid foam was reproduced.

The model presented in this study was very simplified to capture specific features. As a next-step work, physical consideration using thermodynamics and fluid dynamics for the liquid form should be accounted for. Phase transformation from liquid to solid is also required for applying the model to metal foam processing because solidification contraction might induce deformation or destruction. Validation of parameters and comparison of the results with experimental data are also necessary for more precise evaluation of the model. The author has developed another computational model to investigate the stable shape of polyhedral nanoparticles [16]. The application of such an evaluation of polyhedral shapes is also a prospective consideration. Nevertheless, this model may be applied to a wide variety of phenomena because of its simplicity and expandability.

Conflicts of Interest

The author declares no conflicts of interest regarding the publication of this paper.

References

[1] Liu. P.S. and Chen, G.F. (2014) Porous Materials: Processing and Applications. Tsinghua University Press.

[2] Gibson, L.J. and Ashby, M.F. (1988) Cellular Solids: Structure and Properties. Cambridge University Press.

[3] Ashby, M., Evans, A., Fleck, N., Gibson, L., Hutchinson, J., Wadley, H., *et al.* (2001) *Metal Foams: A Design Guide. Applied Mechanics Reviews*, **54**, B105-B106. https://doi.org/10.1115/1.1421119

[4] Kulshreshtha, A. and Dhakad, S.K. (2020) Preparation of Metal Foam by Different Methods: A Review. *Materials Today: Proceedings*, **26**, 1784-1790. https://doi.org/10.1016/j.matpr.2020.02.375

[5] Aste, T. and Weaire, D. (2008) The Pursuit of Perfect Packing. Taylor & Francis.

[6] Saye, R.I. and Sethian, J.A. (2013) Multiscale Modeling of Membrane Rearrangement, Drainage, and Rupture in Evolving Foams. *Science*, **340**, 720-724. https://doi.org/10.1126/science.1230623

[7] Bae, J., Lee, K., Seo, S., Park, J.G., Zhou, Q. and Kim, T. (2019) Controlled Open-Cell Two-Dimensional Liquid Foam Generation for Micro- and Nanoscale Patterning of Materials. *Nature Communications*, **10**, Article No. 3209. https://doi.org/10.1038/s41467-019-11281-y

[8] Guidolin, C., Mac Intyre, J., Rio, E., Puisto, A. and Salonen, A. (2023) Viscoelastic Coarsening of Quasi-2D Foam. *Nature Communications*, **14**, Article No. 1125.

https://doi.org/10.1038/s41467-023-36763-y

[9] Weaire, D. and Phelan, R. (1994) A Counter-Example to Kelvin's Conjecture on Minimal Surfaces. *Philosophical Magazine Letters*, **69**, 107-110. https://doi.org/10.1080/09500839408241577

[10] Weaire, D. and Hutzler, S. (2000) The Physics of Foams. Oxford University Press.

[11] Uehara, T. and Suzuki, H. (2012) Numerical Simulation of Homogeneous Polycrystalline Grain Formation Using Multi-Phase-Field Model. *Applied Mechanics and Materials*, **197**, 628-632. https://doi.org/10.4028/www.scientific.net/amm.197.628

[12] Uehara, T. (2014) Numerical Simulation of Foam Structure Formation and Destruction Process Using Phase-Field Model. *Advanced Materials Research*, **1042**, 65-69. https://doi.org/10.4028/www.scientific.net/amr.1042.65

[13] Uehara, T. (2015) Phase-field Modeling for the Three-Dimensional Space-Filling Structure of Metal Foam Materials. *Open Journal of Modelling and Simulation*, **3**, 120-125. https://doi.org/10.4236/ojmsi.2015.33013

[14] Steinbach, I., Pezzolla, F., Nestler, B., Seeßelberg, M., Prieler, R., Schmitz, G.J., *et al.* (1996) A Phase Field Concept for Multiphase Systems. *Physica D*: *Nonlinear Phenomena*, **94**, 135-147. https://doi.org/10.1016/0167-2789(95)00298-7

[15] Steinbach, I. and Pezzolla, F. (1999) A Generalized Field Method for Multiphase Transformations Using Interface Fields. *Physica D*: *Nonlinear Phenomena*, **134**, 385-393. https://doi.org/10.1016/s0167-2789(99)00129-3

[16] Uehara, T. (2021) Simulation of Polyhedral Crystal Growth Based on the Estimated Surface Energy of Crystallographic Planes. *Materials Sciences and Applications*, **12**, 519-533. https://doi.org/10.4236/msa.2021.1211034